Removal of Inclusions and Trace Elements from Al-Mg-Si Alloys Using Refining Fluxes

Uroš Kovačec¹,², Franc Zupanič¹ ⊠

- 1 University of Maribor, Faculty of Mechanical Engineering, Slovenia
- 2 Impol 2000 d.d., Slovenia

□ franc.zupanic@um.si

Abstract The cleanliness of aluminium alloys has a decisive effect on their properties and performance. In this work, the melts of several Al-Mg-Si alloys (6xxx series) were refined using rotary flux injection (RFI) of the salt fluxes in the industrial environment. A typical charge consisted of 25 % to 30 % external scrap, 45 % to 50 % internal scrap, and 20 % to 30 % primary aluminium. During injection, the entire melt volume was mixed uniformly. The melt was filtered using a porous ring filtration apparatus. The fraction and type of non-metallic inclusions were determined using light and scanning electron microscopy. The contents of alkali and alkaline-earth metals were determined using optical emission spectroscopy. The reduction of alkali and alkaline earth metals and the fraction of non-metallic inclusions were used to evaluate the process efficiency and the flux selection for the regular production. An analysis of more than 100 industry charges confirmed that the flux selected after the experimental trials, consisting of a mixture of MgCl₂, KCl, NaCl and CaF₂, was effective in regular production.

Keywords aluminium, refinement, flux, cleanliness, non-metallic inclusion, rotary injection, alkali element

Highlights

- Alloys were produced with an increased fraction of scrap.
- Melt cleaning was carried out using several salt fluxes.
- Systematic testing in an industrial environment using a rotary flux injection (RFI) system.
- Determination of non-metallic inclusions using porous disc filtration apparatus.
- Optimal removal of non-metallic inclusions and alkali elements by complex fluxes.

1 INTRODUCTION

Al-Mg-Si alloys, which belong to the 6xxx series, are used widely in the automotive, aerospace, and construction industries, due to their excellent combination of properties. They have medium to high strength, good corrosion resistance, and excellent weldability [1]. They also have low density, and can be produced at moderate cost. They are suitable for extrusion processes, making them appropriate for manufacturing structural profiles and components, but they can be deformed using other forming technologies. An essential advantage of Al-Mg-Si alloys is their ability to undergo precipitation hardening, enhancing their mechanical properties considerably, such as strength and hardness, while preserving ductility and toughness [2]. Compared to other aluminium alloys, they offer a balanced combination of strength, ductility, fatigue and corrosion resistance, making them versatile for various applications.

The production of primary aluminium is highly energy-intensive; thus, the use of aluminium scrap instead of primary aluminium can save up to 95 % of energy [3]. Therefore, it is imperative for the new alloys to be produced with an ever-higher addition of aluminium scrap. The scrap fraction represents about 25 % of aluminium production in 2025, and is expected to rise to 50 % by 2050 [4]. For environmental conservation and cost reduction, it is desirable that recycled alloys retain their properties, even after multiple recycling cycles. However, in real life, different adverse effects arise when the scrap fraction is increased [5]. Oxides, paintings and other coatings can cover the surface of scrap, being a source of non-metallic inclusions and residual elements for newly manufactured alloys, worsening their properties gradually [6].

While preparing an aluminium alloy for casting, non-metallic inclusions can come into the melt from several sources. Metallic oxides on the scrap, debris from the furnace lining and agglomerates of borides in Al-Ti-B grain refiners represent the exogenic inclusions. The interaction of the melt with the surroundings, e.g., oxidation with air or reduction of water vapor, can lead to the formation of endogenic inclusions. The reaction with moisture forms aluminium oxide, introducing hydrogen into the melt simultaneously, resulting in several harmful effects [7]. Besides non-metallic inclusions, the amounts of undesired alkali or alkaline earth elements, such as Na and Ca, increase with repeated recycling.

One of the most important approaches to improving the cleanliness of aluminium melts is the application of solid salt fluxes [8]. Solid salt fluxes are mixtures of inorganic compounds, mainly chlorides and fluorides. They are used when processing molten metal, including aluminium recycling, dross treatment and molten metal treatment. Salt fluxes are also added to ensure high metal recovery and decrease oxidation and metal losses [9]. Additionally, salt fluxes are used to treat both primary and secondary molten aluminium, to remove impurities such as alkali and alkaline earth metals and oxides [10]. Chloride and fluoride fluxes in aluminium refining can lead to harmful gaseous emissions, including organochlorine compounds and toxic solid slags, which can have a negative impact on the environment and workers' safety [11]. The effect can be reduced considerably by appropriate measures in the melting plant and the use of the minimum necessary quantity of fluxes, reducing the emissions to the surroundings.

Fluxes can be introduced to aluminium melts using several methods. They can be added by manual application. The powder fluxes are sprinkled onto the surface of the molten aluminium and

stirred into the melt using a tool. Some fluxes, like degassing or grain refining, are plunged to the bottom of the melt; they are typically in the form of tablets or briquettes. The powdered or granulated fluxes can be injected with an inert gas, such as argon or nitrogen. They can also be added by a rotary degasser, which is one of the most effective methods. A rotary degasser injects the flux into the melt while stirring, ensuring thorough mixing [4]. Generally, each method can be used for the introduction of different types of fluxes (cover, dross or melt cleaning fluxes). It depends on the technology which is used in a specific aluminium cast shop. However, each technology has a preferred type of flux. Rotary flux injection (RFI) typically uses granulated fluxes.

Most experiments on applying salt fluxes using RFI are conducted in a laboratory environment [12,13]. There has been no systematic research in an industrial environment yet. Some articles report general principles about mechanisms and applications [14]. This work investigates the application of several compositions of solid salt fluxes systematically on the type and amounts of non-metallic inclusions and residual alkali and alkaline earth elements in Al-Mg-Si alloys using RFI. The analyzes were done using up-to-date industrial equipment and advanced laboratory techniques, such as porous disc filtration apparatus (PoDFA), spectral chemical analysis, light and electron microscopy and microchemical analysis. The main goal of the research was to test different types of fluxes, and then, according to the experimental results, select the optimal flux for regular production.

2 METHODS AND MATERIALS

Several Al-Mn-Si alloys were tested, mainly EN AW 6082, EN AW 6182, and EN AW 6063. They varied slightly in chemical composition. However, all compositions fit inside the tolerances given in Table 1. No specific differences were observed in the behavior of these alloys in the molten state.

Table 1. Range of chemical compositions of the investigated Al-Mn-Si alloys (in wt.%)

Si	Fe	Cu	Mn	Mg	Cr	Zn	Ti	Pb	Zr
1.20	0.25	0.05	0.55	0.80	0.12	0.2	0.05	0.05	0.00
1.30	0.23	0.1	0.70	0.90	0.15				0.15

Several charges were melted in a 50 t multi-chamber gas furnace (SMS-Hertwich Engineering GmbH, Germany). A typical charge consisted of 25 % to 30 % external scrap, 45 % to 50 % internal scrap and 20 % to 30 % primary aluminium. The final temperature achieved in the melting furnace was 750 °C. The melt (26.5 t) was transferred to a one-chamber casting furnace (Sistem Teknik, Turkey), where the required chemical composition was achieved by adding clean master alloys.

The next step was cleaning and refining the melt by using several solid salt fluxes (Table 2). The temperature in the casting furnace during flux treatment was 750 ± 10 °C.

Table 2. Chemical composition of the fluxes (mole and weight fraction in %)

Designation	Chemical composition				
Salt#1	60 % MgCl ₂ , 40 % KCl (weight 54 % MgCl ₂ , 46 % KCl)				
Salt#2	51 % MgCl ₂ , 49 % KCl (weight 45 % MgCl ₂ , 55 % KCl)				
Salt#3	36 % to 40 % MgCl ₂ , 21 % to 26 % KCl, 26 % to 31 % NaCl, 1 % to 3 % CaF ₂ (weight 33 % MgCl ₂ , 26 % KCl, 39 % NaCl, 2 % CaF ₂)				
Salt#4	30 % to 35 % MgCl ₂ , 60 % to 65 % KCl, 1 % to 3 % NaCl, 1 % to 3 % CaF ₂ (weight 27 % MgCl ₂ , 68 % KCl, 3 % NaCl, 2 % CaF ₂)				

The compositions of the salt fluxes were selected based on their melting points, reactivity for removing alkali and alkaline earth elements, density, and their ability to reduce surface tension between the aluminium melt and the molten fluxes. The starting point was the ternary diagram KCl-NaCl-MgCl₂ [15]. The primary agent for removing alkali elements is MgCl₂. Its melting point is too high (714 °C) to be added alone in the Al-melt, because its viscosity is too high at 750 °C. Thus, Salt#1, 40 % KCl, was added to achieve the eutectic composition, with the eutectic temperature of 467 °C, much lower than the temperature of the alloy melt. The second composition, Salt#2, corresponded to the compound KCl MgCl₂, having a slightly higher melting point of 487 °C. Salt#3 lies close to the center of the KCl-NaCl-MgCl2 phase diagram, having as low a melting temperature as 390 °C. Adding NaCl additionally decreases the melting temperature, viscosity and the cost of fluxes because of its much lower price. The Salt#4 had a ternary composition, located close to the binary diagram KCl–MgCl₂ (KCl + MgCl₂ ≈ 95 %) with up to 3 % NaCl and up to 3 % CaF₂, keeping the melting temperature at around 430 °C. The primary role of CaF2 is to reduce the surface tension between the Al-melt and the fluxes, allowing easier separation of both phases.

In each charge, one of the fluxes given in Table 2 was added to the melt. The experimental tests were carried out using fluxes produced by the Hoesch Group and Pyrotek Incorporation, Germany, in the form of granulates up to 3 mm mesh size. The solid salt fluxes (15 kg to 25 kg; 1 kg t⁻¹ melt) were added into a melt using an RFI system (STAS, France) with a feeding rate of 120 kg/h. It is of the utmost importance that the flux is dispersed uniformly in the melt, with as small droplets as possible. The optimal position of the rotor and rotation speed were determined using a mesh-less flow model [16] and experimental testing of the RFI system in the casting furnace. Uniform mixing of the melt can be achieved with the rotor angle of 45° and the rotation speed of 410 min⁻¹, using a graphite impeller with a 400 mm diameter. During mixing, argon was used for the degassing, with a flow rate of 200 L/min.

After fluxing, the melt was grain refined with AlTi3B1 feeding wire, to achieve 0.025 wt.% to 0.030 wt.% Ti in the melt. The melt was then transferred to the degassing unit (Siphon Inert Reactor (SIR), Hycast, Norway) and filtered using a 50 pores per inch ceramic foam filter (CFF). Finally, the alloy was cast into billets with hot-top, air-slip technology [17]. The diameter of the billets was 279 mm.

The alloy cleanliness was tested using different methods. The primary method was PoDFA by ABB, Switzerland [18]. A sample of the molten metal was taken from the melt 30 min after finishing the flux injection and filtered through a porous refractory disc to capture the inclusions. The sample was then prepared by grinding and polishing. The captured inclusions were analyzed using a light microscope (Axio Observer, Zeiss, Germany) and a scanning electron microscope (SEM Jeol JSM 6610LV, Jeol, Japan) equipped with an energy dispersive spectrometer (EDS) to determine their type and content. This method provided both qualitative and quantitative data on the inclusions. The quantitative value is obtained by measuring the area of the inclusions, which is then divided by the mass of the filtered melt. Thus, the unit was mm²/kg.

The chemical analysis of the alloy, including the contents of alkali elements (Na, Ca), was carried out using Spectro S101, SPECTRO Analytical Instruments GmbH, Germany. The light microscopy (LM) and scanning electron microscopy (SEM) samples were ground mechanically using SiC papers with granulations 320 to 4000 and polished using 9 mm, 6 mm and 3 mm diamond paste. The EDS analyzes were carried out using polished samples, while LM required chemical etching with Weck's reagent, consisting of 2 g KMnO₄, 1 g

NaOH, and 50 mL of distilled water. The grain size of the cast billets was determined according to Standard ASTM E112-24 [19].

3 RESULTS AND DISCUSSION

3.1 Microstructure

The alloys solidified in the metallic mold. Without a grain refiner addition, columnar grains of the aluminium solid solution α -Al would grow from the mold walls towards the billet center. The solidification front pushes non-metallic inclusions and alloying elements to the billet center, strongly reducing the alloy's ductility, toughness and malleability. The addition of an effective grain refiner induces heterogeneous nucleation of the α -Al grains throughout the melt, causing the formation and growth of equiaxed crystal grains, which have a typical dendritic morphology. Fig. 1 shows a typical microstructure in the as-cast condition, at lower magnification. It consists of dendritic equiaxed grains of the aluminium solid solution, with a linear intercept length of 200 ±30 μm. Such a small and uniform grain size was obtained by adding the AlTi₃B1 grain refiner. Small equiaxed grains prevent stronger macrosegregations of the alloying elements, allow more uniform distribution of the nonmetallic inclusions and provide improved mechanical properties. Only extremely large non-metallic inclusions can be observed in such micrographs. The grain refiner contains particles of Al₃Ti and TiB₂. Only a small part of the particles causes the heterogeneous nucleation of α-Al crystal grains. Undissolved and inactive TiB₂ particles often form agglomerates, which constitute part of the non-metallic inclusions.

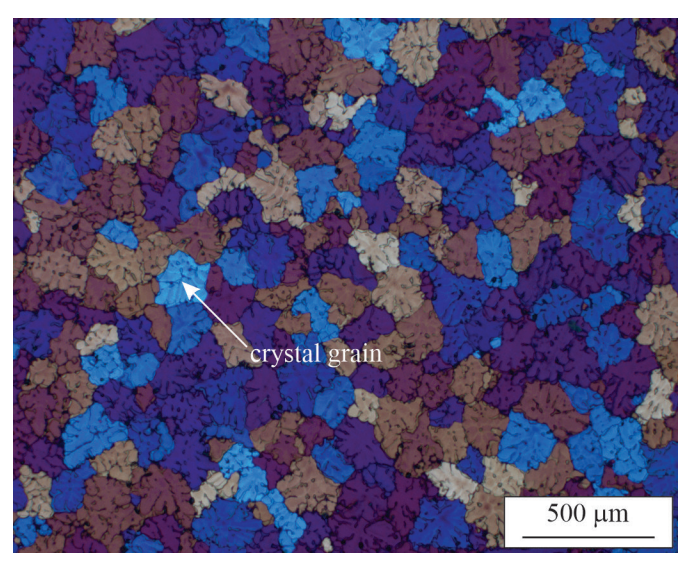
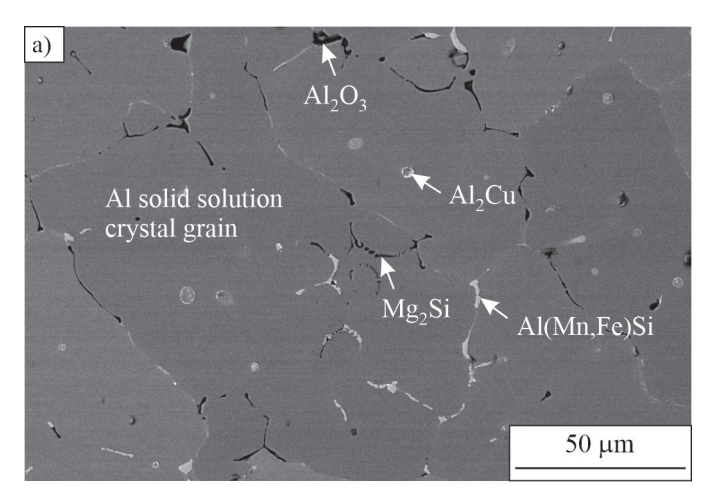
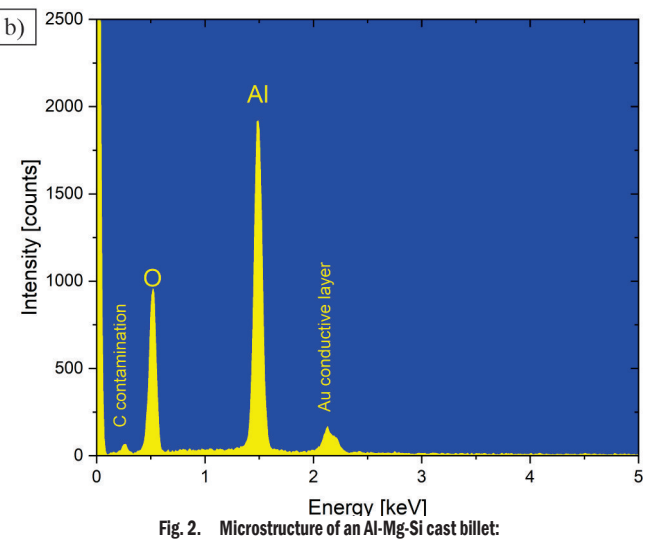


Fig. 1. The grain structure of an Al-Mg-Si cast billet (light micrograph,, depicting each grain in a different color)

Several processes occur during the solidification of Al-Mg-Si alloys. These processes lead to the formation of several other phases. The fractions of these phases are typically no more than a few per cent [20]. Figure 2a shows a SEM micrograph, revealing the dendritic shapes of the aluminium solution grain α -Al. Other phases are located in the interdendritic regions. We identified Al₂Cu, Mg₂Si and α -Al(Mn,Fe)Si phases, which are typical constituents of Al-Mg-Si alloys [2]. Oxide non-metallic inclusion Al2O₃ was identified with EDS analysis (Fig. 2b). It is challenging to find oxide particles, because they appear dark in the backscattered electron images, such as shrinkage porosity, gas porosity and Mg₂Si.

Therefore, much meticulous work is required to obtain adequate results.





a) backscattered electron image, and b) EDS-spectrum of the oxide inclusion

3.2 Non-Metallic Inclusions

Using the PoDFA method, non-metallic inclusions in the melt become concentrated in the filter. Thus, it is possible to identify their types and quantities more easily, even with LM. SEM is used when identification with a light microscope is insufficient. Figure 3 shows a typical light micrograph of non-metallic inclusions before and after melt treatment with fluxes. There are several types of inclusions. The Spinel comes from the furnace lining, while the ${\rm TiB_2}$ was part of the Al-Ti-B grain refiner present in the scrap. On the other hand, ${\rm Al_4C_3}$ is formed by the reaction of Al melt with organic substances [21], and MgO with the dissolved magnesium and oxygen from the atmosphere.

Table 3 gives the results of the quantitative PoDFA analysis. The agglomerated ${\rm TiB_2}$ particles, arising from the grain refiner debris (GF) in the scrap, present the largest fraction of the non-metallic inclusions. Thus, the results for all inclusions and the inclusions without grain refiner debris are given separately. The inclusion fraction was always higher before the melt treatment, indicating the efficiency of the fluxes.

Figure 4 shows the fractions of the non-metallic inclusions after melt treatment in dependence on their fraction before melt treatment. Fig. 4a indicates the effect of individual fluxes. Still, Fig. 4b shows

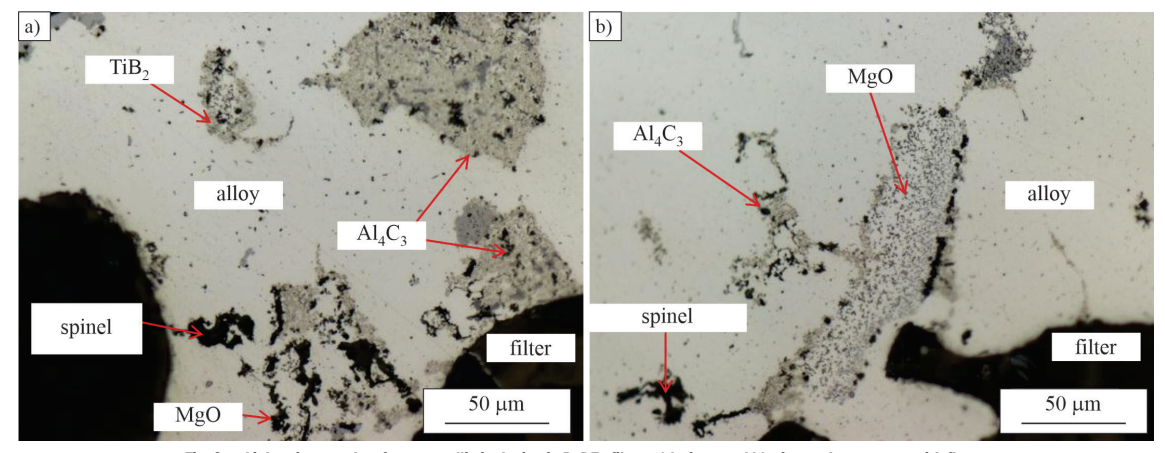


Fig. 3. Light micrographs of non-metallic inclusion in PoDFa filter; a) before, and b) after melt treatment with fluxes

Table 3. Contents of non-metallic inclusions, determined using PoDFA

	Total before [mm²/kg]	Total after [mm²/kg]	Reduction [%]	Without GF before [mm²/kg]	Without GF after [mm ² /kg]	Reduction [%]
Salt#1	1.05	0.37	64.76	0.69	0.32	53.62
Salt#1	0.58	0.29	50.00	0.32	0.14	56.25
Salt#1	0.34	0.05	86.01	0.26	0.04	86.59
Salt#2	2.76	0.75	72.94	2.18	0.50	76.91
Salt#2	1.39	0.34	75.18	1.04	0.20	80.48
Salt#3	0.78	0.10	87.50	0.64	0.01	98.60
Salt#3	1.80	0.14	92.16	1.20	0.20	83.18
Salt#3	1.88	0.69	63.40	1.35	0.50	62.84
Salt#4	3.13	1.11	64.56	2.00	0.62	69.00

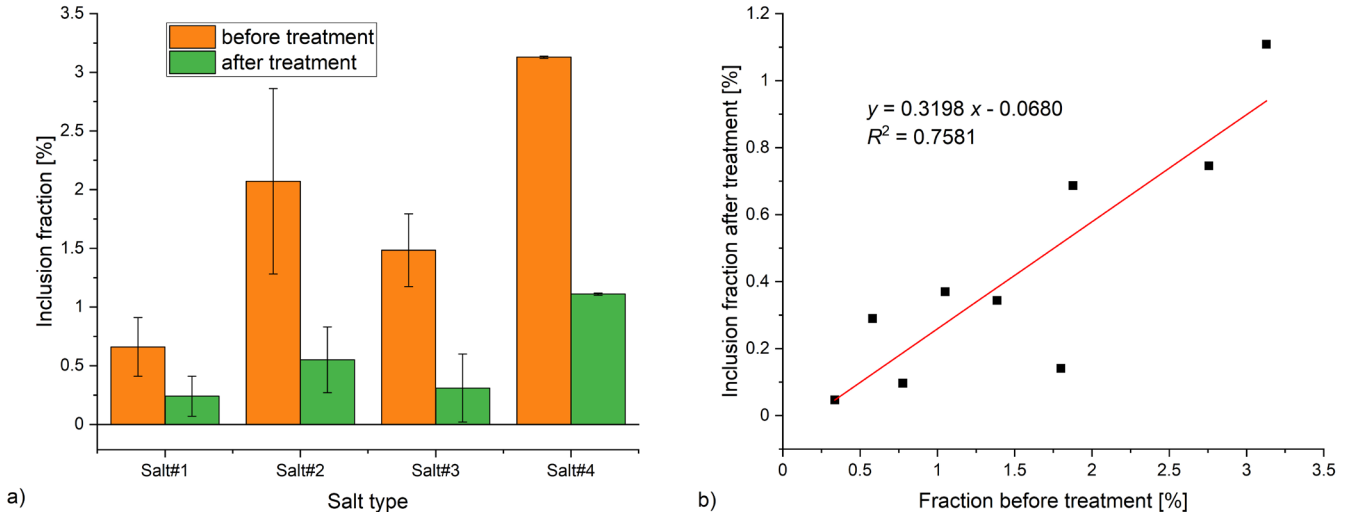


Fig. 4. Inclusions determined using PoDFa; a) the effect of different fluxes (average values from Table 3), b) effectiveness irrespective of the flux type

that the amount of non-metallic inclusion after melt treatment depends strongly on the initial fraction, and that, in each case, the reduction of non-metallic inclusions was about 70 %. Due to the small number of experiments and additional variables occurring in the industrial environment, the scattering was relatively high $(R^2 \approx 0.75)$. Nevertheless, the complex salt mixture Salt#3 was the most efficient (Fig. 4a). One of the reasons can be the presence of CaF₂, which reduces the surface tension and makes the removal of redundant fluxes easier [4]. However, removing inclusions does not depend primarily on the melt treatment with fluxes. The holding time can contribute to better removal of inclusions, because they can have sufficient time either to sink to the furnace bottom or float to

the melt surface, depending on their density (Stoke's law). However, the added fluxes could also stay in the aluminium melt, increasing the fraction of non-metallic inclusions [22]. The PoDFA analysis did not confirm their presence. In industrial practice, the melt is filtered just before casting to reduce the fraction of non-metallic inclusions [23]. However, the melt should contain as few inclusions as possible before filtering, because they can block the filter.

3.3 Removal of Trace Elements

One of the main functions of fluxes is to remove undesirable trace elements. Trace elements are typically present in tiny quantities, e.g.,

in ppm (parts per million), which is equivalent to 10^{-4} %, but can deteriorate the mechanical and other properties of aluminium alloys substantially [24]. Among them, alkali (Li, Na, K, Rb, Cs and Fr) and alkaline earth (Be, Mg, Ca, Sr, Ba and Ra) are very often present in Al-alloys. Mg is one of the most important alloying elements in Al-Mg-Si alloys. The chemical analyzes of all the investigated charges showed that the contents of all the aforementioned elements, except for Na and Ca, were negligible, often below their detection limits. Thus, they could not be used to evaluate the efficiency of the fluxes. Even the maximum contents of Na and Ca were very low, namely, seven ppm $(7\times10^{-4}$ %) and 14 ppm $(14\times10^{-4}$ %), respectively.

Table 4. Contents of Na and Ca using spectroscopic analysis

	Na	Na	Na	Ca	Ca	Ca
	before	after	reduction	before	after	reduction
	[ppm]	[ppm]	[%]	[ppm]	[ppm]	[%]
Salt#1	3.1	2.2	29.0	9.8	4.6	53.1
Salt#1	4.1	2.5	39.0	9.4	5.4	42.6
Salt#1	2.1	1.1	47.6	8.5	4.1	51.8
Salt#1	2.9	1.6	44.8	10.6	3.7	65.1
Salt#1	2.7	1.7	37.0	14.0	5.2	62.9
Salt#1	3.9	1.8	53.9	13.7	4.3	68.6
Salt#2	2.0	2.0	0.0	7.5	2.0	73.3
Salt#2	7.0	2.0	71.4	11.0	3.7	66.4
Salt#3	3.0	2.7	10.0	12.0	1.9	84.2
Salt#3	2.0	1.0	50.0	5.0	1.0	80.0
Salt#3	2.7	0.3	89.1	14.0	0.29	97.9
Salt#4	3.0	1.3	56.7	11.0	3.0	72.7

The results are depicted in Table 4 and Fig. 5. The Salt#3 and Salt#4 removed Na the most effectively. Since the overall content of Na was very low, the effect was not very pronounced (Fig. 5a). On the other hand, it can be seen easily that the Salt#3 was the most potent in removing Ca from the melt (Fig. 5b).

Chloride salt MgCl₂ plays the most crucial role in removing Na and Ca. In the melt, the following chemical reactions take place [25]:

$$MgCl2(I) + 2[Na] \rightarrow 2NaCl(I) + [Mg], \tag{1}$$

$$MgCl_2(l) + [Ca] \rightarrow CaCl_2(l) + [Mg],$$
 (2)

where (l) means the liquid state, and the parentheses [] the dissolved element in the Al-melt.

The free energies of reactions in Eqs. (1) and (2) are hugely negative (ΔG_0) , having a very high equilibrium reaction constant K_p , that can be calculated using Eq. (3).

$$\Delta G_0 = -RT \ln(K_p),\tag{3}$$

where R is the gas constant and T is the absolute temperature.

The actual reaction constant for the reaction in Eq. (1) is calculated as:

$$K = \frac{a_{\text{NaCl}}^2 \cdot a_{\text{Mg}}}{a_{\text{MgCl}_2} \cdot a_{\text{Na}}^2},\tag{4}$$

where a stands for activity. Due to the low values of Na and Mg, activities can be replaced by their concentrations.

The reaction takes place all the time as $K < K_p$. With the addition of the flux in the range of 1 kg per 1 t melt, and the amounts of Na and Ca typical in the industry practice, the reactions do not stop, and can cause a considerable decrease of Na and Ca in the melt.

Figure 5 shows clearly that the amounts of Ca and Na are practically independent of the initial content in the investigated range. It is obvious that the flux Salt#3 can decrease the quantity of Ca below two ppm, very often below one ppm. Since the typical

allowed content of Ca is 20 ppm, the effectiveness of all fluxes was satisfactory. Nevertheless, Salt#3 was selected to be used in industrial applications for the Al-Mg-Si alloys.

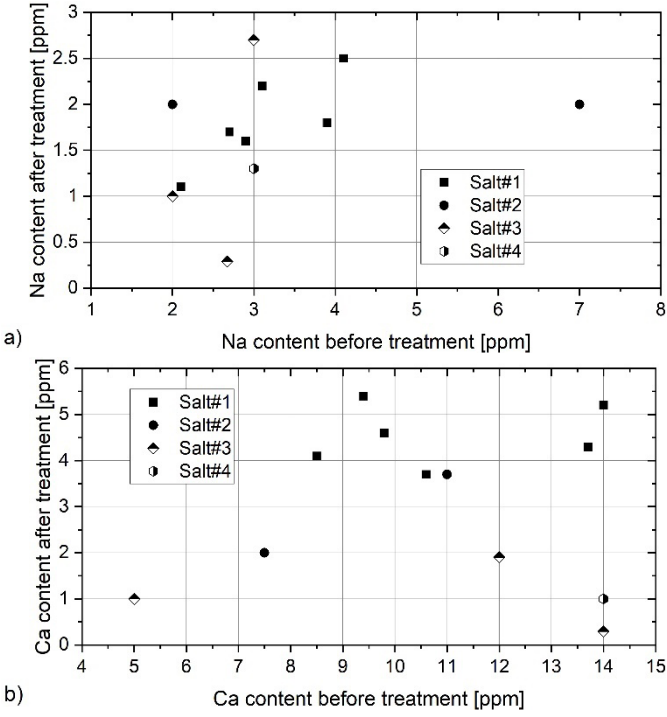


Fig. 5. The effect of different fluxes on the removal of; a) an alkali element, Na, and b) an alkaline earth element, Ca

3.4 Analysis of the Actual Charges

The industrial trials presented above can be considered experimental, because different fluxes were added to Al-Mg-Si alloys in order to select a composition which removes non-metallic inclusions and trace elements effectively from the aluminium melt, and is also cost friendly. After selecting Salt#3, it has been used in regular production.

This part shows the analysis of more than 100 charges of just one alloy EN AW 6182, which is produced in large quantities, so the number of charges is statistically relevant. The chemical analysis was taken after the melting of the alloy and after casting. The only possibility of removing Na and Ca was by melt treatment using the selected flux. All the other treatments can contribute to an increase in these two elements. In many of the investigated charges, the initial contents of Na and Ca were much higher than during the experiments. The highest contents of Na and Ca were 27 ppm and 73 ppm, respectively, thus representing tougher conditions for their removal.

In Fig. 6a, only two charges with less than five ppm Na are shown, indicating the final content of Na below its detection limit. All the other charges (50 charges) contained more than five ppm. The maximum content of Na in the cast billets was three ppm. It was higher only in three charges, suggesting inappropriate handling of the melt in these cases. Only charges with nine or more ppm Ca were selected (70 charges) for the analysis (Fig. 6b). The Ca-content was higher than six ppm only in five charges, showing the efficiency of the Ca removal. It is to be stated that the data for Fig. 6 were shown only for charges having a higher content of Na and Ca. The thermodynamic considerations using Eq. (4) indicate that the final content of harmful trace elements should be independent from their initial content. However, the results of the chemical analyzes in Fig. 6 show a slight dependence on the initial content for both Na and Ca.

Thus, one can expect that also the kinetics of reaction and handling of the aluminium melt can affect the final content of trace elements.

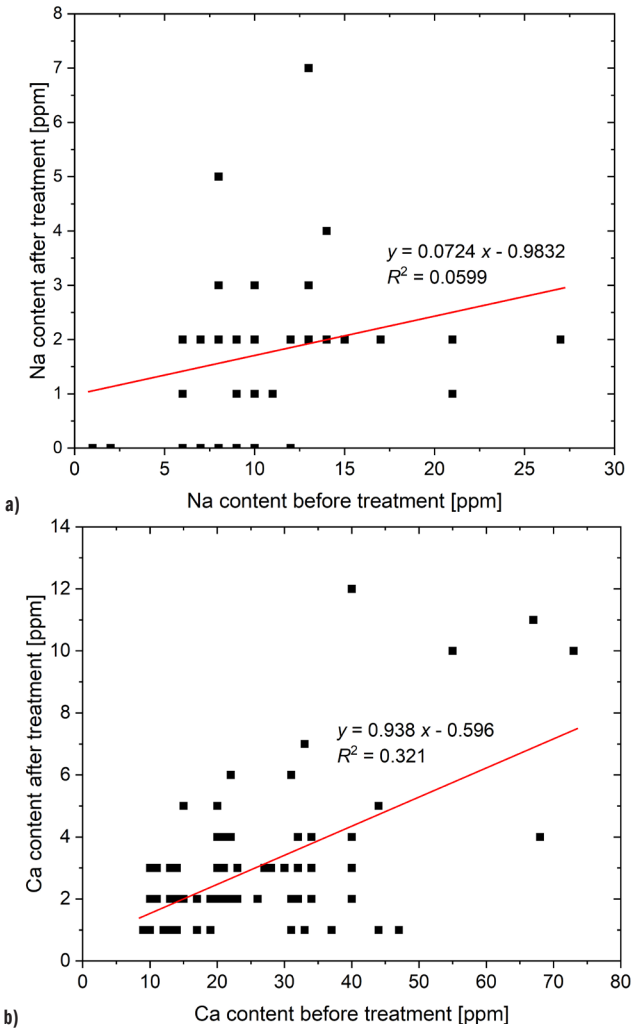


Fig. 6. Removal of Na and Ca from the melt in the actual industrial production;
a) the removal of Na, b) the removal of Ca

The industrial production of aluminium alloys is a highly complex technology. Already in the near future more and more additional parameters will be monitored during production, delivering a lot of data. It is expected that it will be necessary to apply different methods of deep learning and artificial intelligence to obtain strong correlations between the processing parameters and final characteristics of the alloys, similar to the application of deep learning in the production of primary aluminium [26] and other applications [27,28]. One of the important areas will be predictions for the removal of non-metallic inclusions and harmful trace elements in aluminium alloys.

4 CONCLUSIONS

The investigation of the effectiveness of different fluxes leads us to the following conclusions:

- The fraction of non-metallic inclusions and the contents of trace elements can be kept at a sufficiently low level after flux treatment of Al-Mg-Si alloy, containing 25 % to 30 % external scrap.
- Using an RFI system allowed adding fluxes into the melt reliably.
- The fractions and types of non-metallic inclusions were determined by analyzing the sample after filtering through a porous ceramic filter.

- Among the possible trace elements, the Na and Ca contents were determined in detail because of their sufficient amount.
- The alkali and alkaline-earth elements were removed most efficiently using a complex salt mixture containing 36 % to 41 % MgCl₂, 21 % to 26 % KCl, 26 % to 31 % NaCl and 1 % to 3 % CaF₂.
- The efficiency of the selected flux in removing Na and Ca was demonstrated by analyzing more than 100 actual charges of the alloy EN AW 6182.

References

- [1] Polmear, I., StJohn, D., Nie, J.F., Qian, M. Light Alloys: Metallurgy of the Light Metals. Elsevier Ltd. Butterworth-Heinemann Oxford (2017) D0I:10.1016/B978-0-08-099431-4.00001-4.
- [2] Zupanič, F., Steinacher, M., Žist, S., Bončina, T. Microstructure and properties of a novel Al-Mg-Si alloy AA 6086. Metals 11 368 (2021) D0I:10.3390/met11020368.
- [3] Wu, Y., Oudshoorn, T., Rem, P. Modelling and optimization of an innovative facility for automated sorting of aluminium scraps. Waste Manag 189 103-113 (2024) D0I:10.1016/j.wasman.2024.08.018.
- [4] Milani, V., Timelli, G. Solid salt fluxes for molten aluminum processing a review. Metals 13 832 (2023) D0I:10.3390/met13050832.
- [5] Capuzzi, S., Timelli, G. Preparation and melting of scrap in aluminum recycling: A review. Metals 8 249 (2018) D0I:10.3390/met8040249.
- [6] Škůrková, K.L., Ingaldi, M. Recycling process of the aluminium cans as an example of the renewable material sources. Adv Mater Res 1001 103-108 (2014) D0I:10.4028/www.scientific.net/AMR.1001.103.
- [7] Puga, H., Barbosa, J., Soares, D., Silva, F., Ribeiro, S. Recycling of aluminium swarf by direct incorporation in aluminium melts. J Mater Process Technol 209 5195-5203 (2009) DOI:10.1016/j.jmatprotec.2009.03.007.
- [8] Máté, M., Tokár, M., Fegyverneki, G., Gyarmati, G. The comparative analysis of the inclusion removal efficiency of different fluxes. Arch Foundry Eng 20 53-58 (2020) D0I:10.24425/afe.2020.131302.
- [9] Damoah, L.N.W., Zhang, L. Alf3 reactive Al203 foam filter for the removal of dissolved impurities from molten aluminum: Preliminary results. Acta Mater 59 896-913 (2011) D0I:10.1016/j.actamat.2010.09.064.
- [10] Gaustad, G., Olivetti, E., Kirchain, R. Improving aluminum recycling: A survey of sorting and impurity removal technologies. Resour Conserv Recyc 58 79-87 (2012) D0I:10.1016/j.resconrec.2011.10.010.
- [11] Brough, D., Jouhara, H. The aluminium industry: A review on state-of-the-art technologies, environmental impacts and possibilities for waste heat recovery. *Int J Thermofluids* 1-2 100007 (2020) D0I:10.1016/j.ijft.2019.100007.
- [12] Piękoś, M., Smorawiński, Z. Introduction of powder fluxes in rotary degassing system towards intensifying refining process of aluminium alloys. Arch Foundry Eng 24 89-94 (2024) DOI:10.24425/afe.2024.151315.
- [13] Wan, B., Chen, W., Mao, M., Fu, Z., Zhu, D. Numerical simulation of a stirring purifying technology for aluminum melt. J Mater Process Technol 251 330-342 (2018) D0I:10.1016/j.jmatprotec.2017.09.001.
- [14] Breton, F., Larouche, A., Waite, P., Côté, P. Rotary flux injector (RFI): Recent development towards an autonomous technology. Hyland, M. (ed.) *Light Metals* Springer International Publishing Cham 901-904 (2016) D0I:10.1007/978-3-319-48248-4 151.
- [15] Villada, C., Ding, W., Bonk, A., Bauer, T. Engineering molten MgCl₂-KCl-NaCl salt for high-temperature thermal energy storage: Review on salt properties and corrosion control strategies. Sol Energy Mater Sol Cells 232 111344 (2021) D0I:10.1016/j. solmat.2021.111344.
- [16] Mramor, K., Vertnik, R., Sarler, B. Meshless approach to the large-eddy simulation of the continuous casting process. Eng Anal Bound Elem 138 319-338 (2022) D0I:10.1016/j.enganabound.2022.03.001.
- [17] Faunce, J.P., Valdo, A. The air-slip casting mold an established technology (reprinted from light-metals, 1985). Light Met Age 43 10-15 (1985).
- [18] Gauthier, P., Bilodeau, V., Sosa, J. A PoDFA benchmarking study between manual and ai-supervised machine learning methods to evaluate inclusions in wrought and foundry aluminum alloys. *Light Metals* (2024) 970-976 D0I:10.1007/978-3-031-50308-5_121.
- [19] E112-24. Standard Test Methods for Determining Average Grain Size. ASTM International West Conshohocken.
- [20] Engler, O., Schröter, T., Krause, C. Formation of intermetallic particles during solidification and homogenisation of two Al-Mg-Si alloys. *Mater Sci Technol* 39 70-84 (2023) D0I:10.1080/02670836.2022.2102279.

- [21] Mendoza-Duarte, J.M., Estrada-Guel, I., Garcia-Herrera, J.E., Perez-Bustamante, R., Arcos-Gutiérrez, H., Martinez-García, A. et al. Aluminum carbide formation in Al-graphite composites: In situ study and effects of processing variables and sintering method. *Mater Today Commun* 38 108396 (2024) D0I:10.1016/j. mtcomm.2024.108396.
- [22] Majidi, O., Shabestari, S.G., Aboutalebi, M.R. Study of fluxing temperature in molten aluminum refining process. J Mater Process Technol 182 450-455 (2007) D0I:10.1016/j.jmatprotec.2006.09.003.
- [23] Kvithyld, A., Syvertsen, M., Bao, S., Eriksen, U.A., Johansen, I., Gundersen, E., Akhtar, S., Haugen, T., Gihleengen, B.E. Aluminium filtration by bonded particle filters. Light Metals (2019) 1081-1088 D0I:10.1007/978-3-030-05864-7_132.
- [24] Casari, D., Ludwig, T.H., Merlin, M., Arnberg, L., Garagnani, G.L. The effect of Ni and V trace elements on the mechanical properties of A356 aluminium foundry alloy in as-cast and t6 heat treated conditions. *Mater Sci Eng A* 610 414-426 (2014) D0I:10.1016/i.msea.2014.05.059.
- [25] Utigard, T. Thermodynamic considerations of aluminum refining and fluxing. Sahoo, M., Pinfold, P. (eds.), Extraction, Refining, and Fabrication of Light Metals. Pergamon (1991) Amsterdam 353-365 D0I:10.1016/B978-0-08-041444-7.50034-2.
- [26] Wang, J., Xie, Y., Xie, S., Chen, X. Optimization of aluminum fluoride addition in aluminum electrolysis process based on pruned sparse fuzzy neural network. ISA Transactions 133 285-301 (2023) D0I:10.1016/j.isatra.2022.06.039.
- [27] Babič, M., Kovačič, M., Fragassa, C., Šturm, R. Selective laser melting: A novel method for surface roughness analysis. 70 12 (2024) D0I:10.5545/svjme.2024.1009.
- [28] Van, A.-L., Nguyen, T.-C., Bui, H.-T., Dang, X.-B., Nguyen, T.-T. Multi-response optimization of gtaw process parameters in terms of energy efficiency and quality. 70 11 (2024) D0I:10.5545/sv-jme.2023.890.

Received: 2025-04-24, revised: 2025-07-04, accepted: 2025-07-17 as Original Scientific Paper 1.01.

Data Availability The data supporting this study's findings are available from the corresponding author upon reasonable request.

Author Contribution Uroš Kovačec: Conceptualization, Data curation, Investigation, Writing – original draft; and Franc Zupanič: Conceptualization, Methodology, Writing – review & editing, Supervision.

Al-Assisted Writing The Al tool Grammarly was used to prepare this manuscript for grammar and language editing. All the content and conclusions remain the responsibility of the authors.

Odstranjevanje vključkov in elementov v sledovih iz zlitin Al-Mg-Si z rafinacijskimi talili

Povzetek Čistoča aluminijevih zlitin ima odločilen vpliv na njihove lastnosti in uporabnost. V industrijskem okolju smo rafinirali taline več Al-Mg-Si zlitin (serija 6xxx) s solnimi talili, ki smo jih vnašali v talino z rotacijskim vpihovanjem. Običajni vložek je bil sestavljen iz 25 % do 30 % zunanjega odpada, 45 % do 50 % notranjega odpada in 20 % do 30 % primarnega aluminija. Talina je bila med vpihovanjem talil enakomerno premešana in nato je bila filtrirana skozi porozni obročasti filter. Za opredelitev deleža in vrste nekovinskih vključkov smo uporabili svetlobno mikroskopijo in vrstično elektronsko mikroskopijo. Z optično emisijsko spektroskopijo je bil izmerjen delež alkalijskih in zemljoalkalijskih kovin. Zmanjšanje deleža alkalijskih in zemljoalkalijskih kovin ter deleža nekovinskih vključkov je bilo merilo za ovrednotenje učinkovitosti rafinacije in za izbiro rafinacijskega sredstva za redno proizvodnjo. Analiza več kot sto industrijskih vložkov je potrdila, da je bilo izbrano talilo, sestavljeno iz zmesi MgCl₂, KCl, NaCl in CaF₂, učinkovito tudi pri redni proizvodnji.

Ključne besede aluminij, rafinacija taline, talilo, čistoča, nekovinski vključek, rotacijsko vbrizgavanje, alkalijski element